ChemSusChem

Research Article
doi.org/10.1002/cssc.202400160

Chemistry Europe
European Chemical Societies Publishing

www.chemsuschem.org

Sulfonated Chitosan Gel Membrane with Confined Amine Carriers for Stable and Efficient Carbon Dioxide Capture

Lixinyu Wang,[a] Shangwen Zha,[c] Shenxiang Zhang,*[a, b] and Jian Jin*[a, b]

Capturing carbon dioxide (CO_2) from flue gases is a crucial step towards reducing CO_2 emissions. Among the various carbon capture methods, facilitated transport membranes (FTMs) have emerged as a promising technology for CO_2 capture owing to their high efficiency and low energy consumption in separating CO_2. However, FTMs still face the challenge of losing mobile carriers due to weak interaction between the carriers and membrane matrix. Herein, we report a sulfonated chitosan (SCS) gel membrane with confined amine carriers for effective CO_2 capture. In this structure, diethylenetriamine (DETA) as a CO_2-mobile carrier is confined within the SCS gel membrane via electrostatic forces, which can react reversibly with CO_2 and thus greatly facilitate its transport. The SCS ion gel membrane allows for the fast diffusion of amine carriers within it while blocking the diffusion of nonreactive gases, like N_2. Thus, the prepared membrane exhibits exceptional CO_2 separation capabilities when tested under simulated flue gas conditions with CO_2 permeance of 1155 GPU and an ultra-high CO_2/N_2 selectivity of above 550. Moreover, the membrane retains a stable separation performance during the 170 h continuous test. The excellent CO_2 separation performance demonstrates the high potential of gel membranes for CO_2 capture from flue gas.

Introduction

With the fast development of modern industry, the combustion of fossil fuels has become the main factor of excessive CO_2 emissions, leading to global warming, ocean acidification and serious damage to the ecological environment.[1] Carbon capture, utilization and storage (CCUS) is considered as the key technologies to combat global climate change. Among numerous carbon capture technologies, membrane separation technology is considered to be a promising technology because of its unique advantages of high separation efficiency, low energy consumption, flexible operation and environmental friendliness.[2]

Polymer membranes are extensively researched for CO_2 separation and capture.[3] However, due to the trade-off between permeability and selectivity, polymer membranes exhibit limited separation efficiency in large-scale CO_2 capture applications. To break through this inherent trade-off effect, there have been many studies on the preparation of mixed matrix membranes (MMMs)[4] by adding nano-fillers, such as covalent-organic frameworks (COFs),[5] metal-organic frameworks (MOFs),[6] porous organic cages (POCs)[7] and zeolite,[8] to the polymer matrix. By combining the high porosity of porous fillers and the excellent machinability of polymers, the permeability of CO_2 and the selectivity of CO_2/N_2 have been significantly improved. However, under flue gas conditions (with temperatures of 50–90 °C and nearly 100 % humidity), high temperature and water vapor may cause aging of the polymer chain and destruction of the nano-filler. Unfortunately, water vapor is commonly present in flue gases, hindering the use of MMMs.

To achieve high CO_2 separation performance under flue gas conditions, facilitated transport membranes (FTMs) have been developed based on the mechanism of immobilized liquid membranes.[9] The mobile carriers are incorporated into the membrane to allow for a reversible reaction with CO_2. The intermediate formed by CO_2 and amine carriers can move rapidly within the FTM. In contrast, the solubility of nonreactive molecules, such as N_2, CH_4, and H_2, in FTM is very low. Therefore, FTM can achieve high CO_2/N_2 selectivity while maintaining high CO_2 permeability. However, the configuration of mobile carriers within FTM is relatively unstable because the carrier agents can be easily washed out during separation, particularly under flue gas conditions with high humidity.[10] Therefore, it is crucial to design a matrix that can simultaneously ensure the rapid transport of carriers and avoid carrier loss during the separation process.

Herein, we designed and fabricated a stable FTM by using sulfonated chitosan (SCS) gel as the matrix. As shown in Figure 1, protonated diethylenetriamine (DETA) as a mobile carrier is firmly confined in SCS gel via intermolecular electrostatic force with the negatively charged sulfonic groups. CO_2 molecules can react reversibly with the mobile carrier to form an intermediate that can rapidly diffuse within the SCS gel. However, nonreactive gas, like N_2, is blocked by the SCS gel membrane. After optimization of the thickness of SCS gel and

---

[a] L. Wang, Dr. S. Zhang, Prof. J. Jin
College of Chemistry, Chemical Engineering and Materials Science, Jiangsu Key Laboratory of Advanced Functional Polymer Design and Application, Soochow University, Suzhou, Jiangsu 215123, China
E-mail: jjin@suda.edu.cn
sxzhang@suda.edu.cn

[b] Dr. S. Zhang, Prof. J. Jin
Collaborative Innovation Center of Suzhou Nano Science and Technology, Jiangsu Key Laboratory of Advanced Negative Carbon Technologies, Soochow University, Suzhou, Jiangsu 215123, China

[c] Dr. S. Zha
Department of Research and Development, Shanghai ECO Polymer Sci.&Tech. CO., Ltd, Shanghai, 201306, China

Supporting information for this article is available on the WWW under https://doi.org/10.1002/cssc.202400160

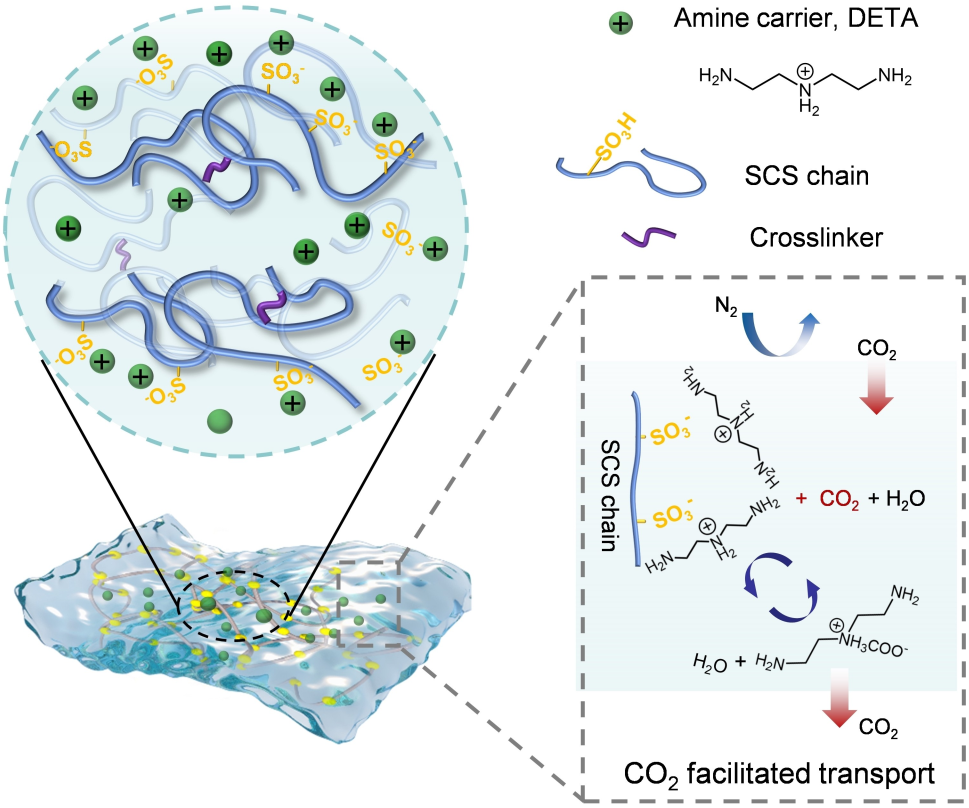

Figure 1. Schematic illustration of the design of SCS-DETA membrane for effective CO_2 separation.

the loading amount of mobile carriers, the resulting membrane, denoted as SCS-DETA, was able to achieve ultra-high CO_2/N_2 selectivity >550 with CO_2 permeance up to 1155 gas permeation units (GPUs, 1 GPU $= 3.348\times10^{-10}$ mol m^{-2} s^{-1} Pa^{-1}) for simulated flue gas, superior to most of the reported post-combustion CO_2 capture membranes. Furthermore, during a continuous test spanning over 170 hours, the SCS-DETA membrane displayed a stable separation performance. This is attributed to the strong electrostatic interaction between the amine carriers and SCS gel matrix. The membrane's high performance and stability indicate its immense potential for practical application in CO_2 capture.

Results and Discussion

Fabrication and Characterization of SCS-DETA Membrane

Figure 2a presents the process of preparing SCS gel. Initially, the SCS solution is a highly viscous liquid. After 20 minutes of crosslinking with glutaraldehyde, it transforms into a stable gel that can be easily removed from the culture dish. The water content of SCS gel is about 92.5 %, indicating a strong water retention ability (Figure S1, Supporting Information). To evaluate the strength of the SCS gel, a solution of SCS with a concentration of 80 mg mL^{-1} was crosslinked and dropped onto a glass plate. After that, it was peeled off and subjected to a tensile test. As a result of the test, it was found that the SCS gel had a tensile strength of 23.2 MPa (Figure S2, Supporting Information), presenting a good mechanical strength.

The chemical structure of SCS gel was studied using ^{1}H nuclear magnetic resonance (^{1}H NMR) spectroscopy. Figure 2b shows distinct peak signals at 1.8, 2.8, and 3.7 ppm, indicating the presence of propyl sulfonic acid groups. The peaks at 3.8, 3.1 and 3.3 ppm belong to the unreacted amine group hydrogen on the chitosan unit and incompletely deacetylated acetyl group. The Fourier transform infrared (FTIR) spectroscopy was used to comprehensively investigate the change in chemical structure before and after sulfonation, including the structure after forming gel. In Figure 2c, we can observe some new peaks at 1141 and 1088 cm^{-1} in SCS gel compared with chitosan (CS), which corresponds to the sulfonic acid group. There are peaks at 790 and 731 cm^{-1} that can be attributed to the $-CH_2-$ unite in propane sulfonic acid groups, indicating that the successful introduction of the propyl sulfonic acid group.

The preparation process of SCS-DETA gel membrane is shown in Figure 3a. To achieve a high CO_2 permanence, a porous carbon nanotube (CNT) network supported by a commercial polyether sulfone microfiltration membrane (PES) was selected as the substrate. The CNT network support layer was firstly prepared on the surface of through a vacuum filtration method according to our previous reports.[11] As shown in Figure S3, scanning electron microscopy (SEM) image shows that CNT are randomly stacked together on the surface of PES microfiltration membrane, forming a network structure with high porosity. The gas permeance of CNT membrane is as high

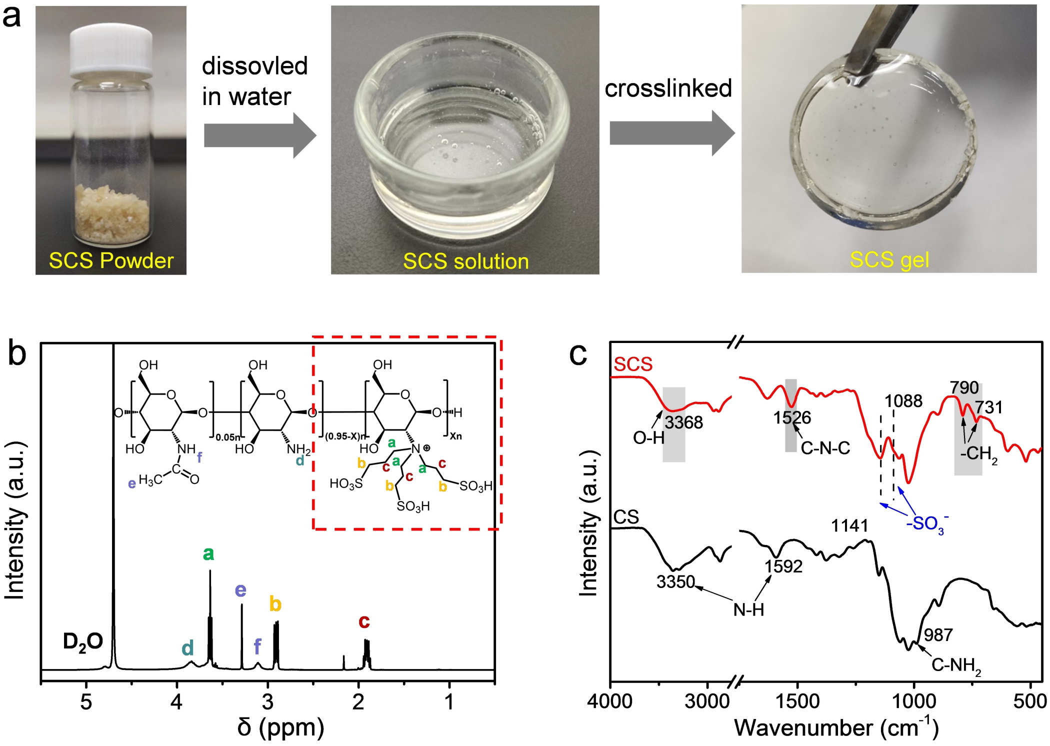

Figure 2. Preparation and characterization of SCS gel. (**a**) Digital photographs of the gelation process of SCS. (**b**) ^{1}H NMR spectrum of SCS. (**c**) FTIR spectra of CS and SCS.

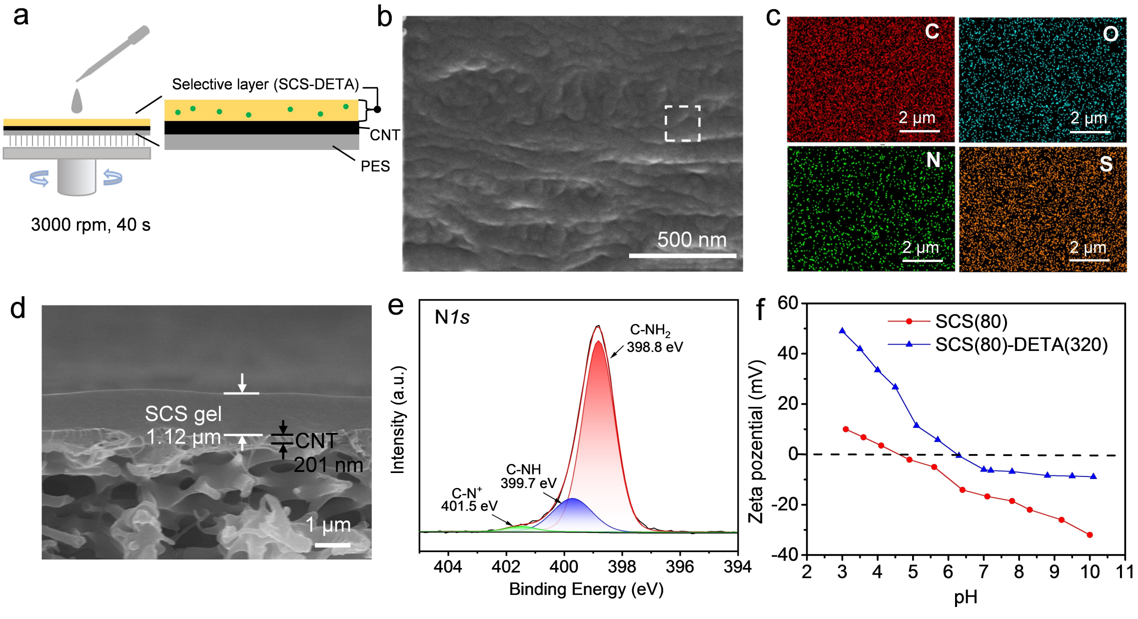

Figure 3. Preparation and characterization of the SCS-DETA membrane. (**a**) Fabrication process and structure diagram of the SCS-DETA membrane. (**b**) Top-view SEM images of SCS-DETA membrane and (**c**) Corresponding elemental mapping images of carbon, oxygen, nitrogen, and sulfur. (**d**) Cross-sectional SEM images of SCS-DETA membranes. (**e**) XPS spectra of SCS-DETA membrane in N 1s region. (**f**) Surface zeta potential of SCS membrane and SCS-DETA membrane.

as 28000 GPU. We attempted to fabricate a SCS gel membrane directly onto a commercial PES ultrafiltration membrane with an effective pore size of approximately 50 nm; however, due to the membrane's low porosity, the gas permeance was roughly 260 GPU. For this work, a PES microfiltration membrane-supported CNT network was selected as the substrate. The CNT network acted as a support for the SCS gel layer, preventing it from penetrating into the PES substrate. Then SCS gel was deposited on the CNT support layer by spin coating. A gel layer was formed on the surface of the membrane (Figure 3b, 3d and

Figure S4, Supporting Information). After forming a SCS gel network, DETA was spin-coated on SCS gel to obtain SCS-DETA membrane. To confirm the successful loading of DETA into the SCS gel layer, we conducted energy dispersive spectrometer-mapping (EDS-mapping) characterization (Figure 3c). Nitrogen content in the SCS-DETA membrane is 18.1 %, higher than that of the SCS membrane (7.3 %, see Table S1, Supporting Information). Figure 2c shows that the elements C, O, N, and S were uniformly distributed in the SCS selective layer. Complementary, we conducted FTIR on the membranes before and after loading DETA. As shown in Figure S5, the new peaks at 3319, 1635, and 815 cm^{-1} appeared in SCS-DETA membrane, which are attributed to the introduction of $-NH_2$. Figure 3e shows the high-resolution X-ray photoelectron spectroscopy (XPS) spectrum of the deconvoluted N 1s of SCS-DETA gel membrane. There are three types of N signals, corresponding to $C-NH_2$ (398.8 eV), C-NH (399.7 eV) and $C-N^+$ (401.5 eV) respectively, indicating that DETA exists as protonation in SCS gel.

In order to verify the electrostatic interaction between sulfonic groups in SCS and protonation amines in DETA, the surface zeta potential of SCS membrane and SCS-DETA membrane were measured respectively (Figure 3f). For SCS membrane, the isoelectric point (IEP) was about 4.55, and their zeta potential was about -16.26 mV in a neutral environment, When the pH increased from 3.1 to 10.0, the surface zeta potential decreased from 10.3 to -32.4 mV, indicating that the abundant sulfonic acid groups in SCS created a strong negatively charged environment. For SCS-DETA membranes, the IEP was approximately 6.3. In a neutral environment, its zeta potential was about -4.8 mV, with weak negative charge, indicating that the negative charge on SCS was partially neutralized by protonated DETA ($DETAH^+$). When pH was lower than the IEP, the zeta potential on the surface of the SCS-DETA membrane increased rapidly, reaching about 50 mV at $pH = 3.1$, which was caused by the combination of unprotonated DETA and H^+, indicating that DETA has a strong protonation ability. These results indicated that the $DETAH^+$ carriers were confined within negatively charged SCS through electrostatic force.

Gas Separation Performance of SCS-DETA Membrane

The CO_2/N_2 separation performance of the membrane was evaluated using a homemade gas permeation apparatus (Figure S6, Supporting Information). The simulated flue gas ($CO_2/N_2 = 10/90$ vol %) entered the membrane cell from the feed side. The sweep gas carried the permeate gas to a gas chromatography (GC) for component analysis. When DETA was directly coated onto the CNT substrate, with no SCS gel, the CO_2/N_2 selectivity decreased quickly. During the one-hour test, the selectivity dropped from 500 to 13 (Table S2), indicating that DETA was gradually losing from the CNT substrate. When SCS spin coating was applied on CNT without DETA, the membrane exhibited CO_2 permeance of about 300 GPU and CO_2/N_2 selectivity of about 400 (Figure 4a). The CO_2/N_2 selectivity is due to amine groups in SCS gel that act as fixed carriers for CO_2 transport. To further enhance CO_2 permeance, DETA as CO_2 mobile carrier, was incorporated into the SCS gel membranes via electrostatic attraction between $DETAH^+$ and negatively charged groups. The SCS-DETA membrane exhibited a CO_2 permeance of 539 and an ultrahigh CO_2/N_2 selectivity, up to 952. Other amine molecules, such as tetraethylenepentamine (TEPA), piperazine (PIP), can be used as mobile carriers. Under optimal conditions, they exhibited a CO_2 permeance of 464, and 360 GPU, respectively, and CO_2/N_2 selectivity of 1094, and 562, respectively (Figure S7, Supporting Information). These results demonstrate that the negatively charged SCS gel layer has an excellent stabilizing effect on amine mobile carriers, promoting the efficient transport of CO_2. Due to the mass transfer resistance of the gel, the transport of nonreactive gas, N_2, is blocked, resulting in ultra-high CO_2/N_2 selectivity.

In order to investigate the influence of SCS gel layer thickness on CO_2/N_2 separation performance, a series of SCS-DETA membranes with different SCS gel layer thickness was prepared by changing SCS concentration from 40 $mg\,mL^{-1}$ to 100 $mg\,mL^{-1}$. It could be observed that with the SCS concentration increasing, the thickness of SCS gel layer increased from 463 nm to 1.49 μm (Figure S8, Supporting Information). Figure 4b shows a linear relationship between SCS concentration and the thickness of the SCS gel layer. This suggests that the thickness of the SCS gel layer can be precisely adjusted by altering the concentration of SCS. An increase in SCS concentration led to a decrease in the radian at the gel-air interface (Figure S9, Supporting Information), indicating a stronger gel structure. The effect of SCS concentration on the separation performance of CO_2/N_2 is shown in Figure 4c. With the SCS concentration increased from 40 to 80 $mg\,mL^{-1}$, CO_2 permeance increased from 459 to 539 GPU, meanwhile, CO_2/N_2 selectivity increased from 500 to 952. When SCS concentration was further increased to 100 $mg\,mL^{-1}$. CO_2 permeance slightly decreased to 520 GPU. These results indicated that a thick SCS gel layer favored confining more amine carriers and thus higher CO_2 permeance. At higher concentrations of SCS, it becomes possible to stabilize more DETA. However, this also affects the separation performance because the thickness of the gel layer increases. As a result, the mass transfer resistance becomes more influential than the facilitated transport effect. Therefore, in order to achieve optimal CO_2 permeance and CO_2/N_2 selectivity, it was imperative to ascertain the optimal SCS concentration. Here, we selected 80 $mg\,mL^{-1}$ as the optimal SCS concentration, where the mass transfer resistance and facilitated transport effect reached equilibrium.

In order to explore the influence of DETA concentration on CO_2/N_2 separation performance, we tuned the loading amount of mobile carriers in SCS gel membrane. Table S1 presents the effect of DETA concentration in casting solution on the amine carrier loading amount in the membrane. The nitrogen content increased from 11.3 % to 18.9 % with the increase of DETA concentration from 40 to 320 $mg\,mL^{-1}$ in the casting solution, suggesting a higher concentration of DETA in the casting solution resulted in a higher amount of carrier loading in the membrane. With DETA concentration increase from 40 $mg\,mL^{-1}$ to 320 $mg\,mL^{-1}$, both CO_2 permeance and CO_2/N_2 selectivity exhibited an increasing trend (Figure 4d). When the concen-

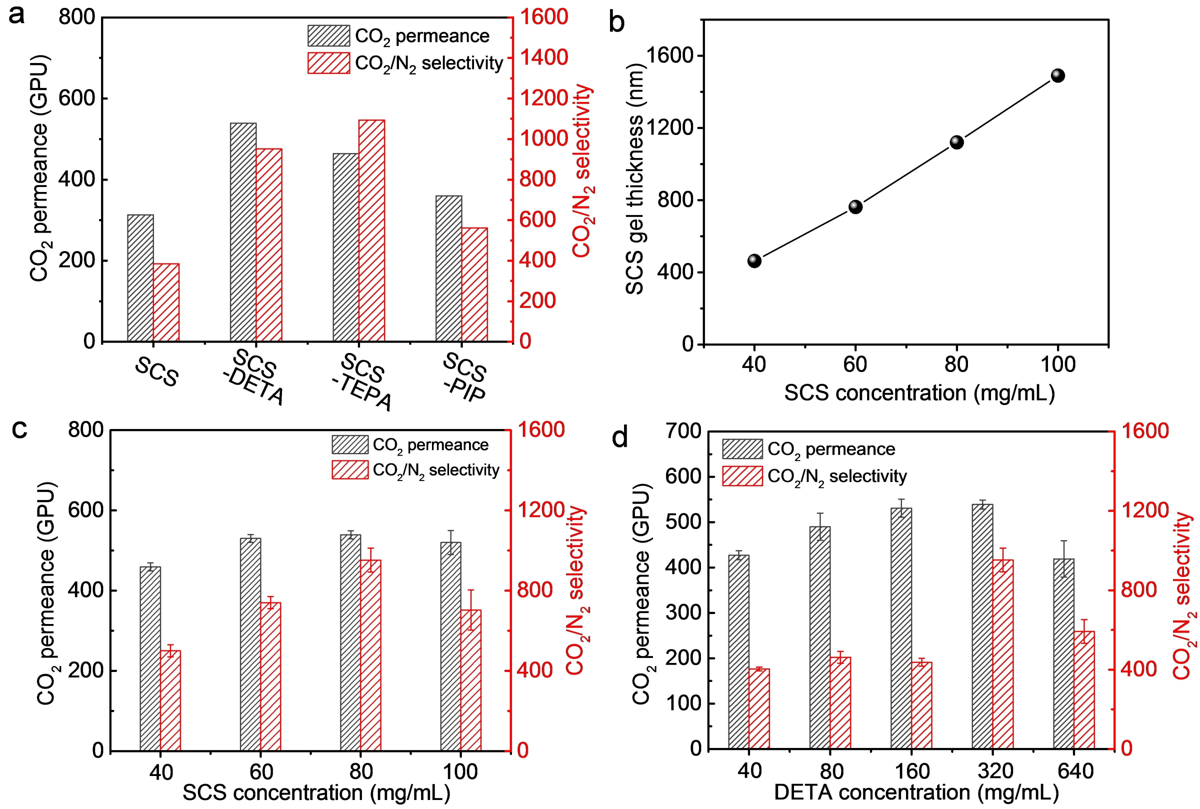

Figure 4. CO$_2$ separation performance. (**a**) Effect of amine carriers on the separation performance of CO$_2$/N$_2$. (**b**) Relationship between thickness and concentration of SCS gel. (**c**) Effect of SCS concentration on CO$_2$ separation performance. (**d**) Effect of DETA concentration on CO$_2$ separation performance. All the membranes were tested at 75 °C with Ar as sweeping gas.

tration of DETA was 320 mg mL^{-1}, the CO$_2$ permeance reached 539 GPU, while the CO$_2$/N$_2$ selectivity reached 952. However, when the DETA concentration further increased to 640 mg mL^{-1}, CO$_2$ permeance and CO$_2$/N$_2$ selectivity decreased to 419 GPU. The decrease in separation performance is possible because the high concentration of DETA led to an increase in viscous resistance, reducing the transfer rate of intermedia formed between DETA and CO$_2$. Therefore, the optimal condition for the following investigation was DETA concentration of 320 mg mL^{-1} in the casting solution.

Gas separation performance of SCS-DETA membranes was investigated at temperatures ranging from 65 to 90 °C (Figure 5a). The CO$_2$ permeance increased exponentially as the temperature increased. At 65 °C, it was 334 GPU. At 75 °C, it increased to 539 GPU, and at 85 °C, it further increased to 810 GPU. Finally, at 90 °C, it reached 1155 GPU. As the temperature increased, the selectivity increased, from 678 at 65 °C to 952 at 75 °C. This was mainly due to the increase in CO$_2$ permeance. However, at 90 °C, the selectivity decreased to 557, probably because N$_2$ diffusion was faster at higher temperatures. CO$_2$ permeance increased exponentially with the increase of temperature and followed an Arrhenius relationship[12] (Figure S10, Supporting Information). The activation energy (E$_a$) of CO$_2$ transport was calculated to be 52.4 kJ/mol, indicating an activated diffusion of CO$_2$ in the SCS-DETA membrane.

In order to evaluate the stability of the prepared SCS-DETA membranes, we operated a long-term test at 85 °C (Figure 5c). The results show that even at a high temperature of 85 °C, the prepared SCS gel membranes can still maintain long-term stability for up to 170 h (fluctuation $<7\%$), with an average CO$_2$ permeance of 730 GPU and an average CO$_2$/N$_2$ selectivity of 700. It far exceeds most of the reported facilitated transport membranes (with long-term stability less than 80 h). In order to further confirm the stabilizing effect of the negative electric group in SCS, we prepared CS gel membranes without sulfonic acid group as a contrast. We found that the CO$_2$ permeance of CS-DETA membrane decreased significantly in the first 10 h, and dropped to less than 50 % of the initial state after 120 h (Figure S11, Supporting Information). This is mainly due to the fact that there was no negative group in CS, and thus, the CS gel alone cannot stabilize DETA. FTIR and EDS results further confirmed the loss of amine carriers in CS gel membrane after the long-term test, while DETA remained relatively stable in the SCS gel membrane (Figure S12, Supporting Information). These results suggest that the DETA carriers should have been confined within the gel membrane by negatively charged sulfonic acid group via electrostatic force.

As a result, the excellent separation performance transcends the 2019 Robeson upper bound[13] for CO$_2$/N$_2$ gas pair (Figure 5b and Table S3, Supporting Information). Meanwhile, the SCS-DETA membranes exhibit a competitive advantage over a

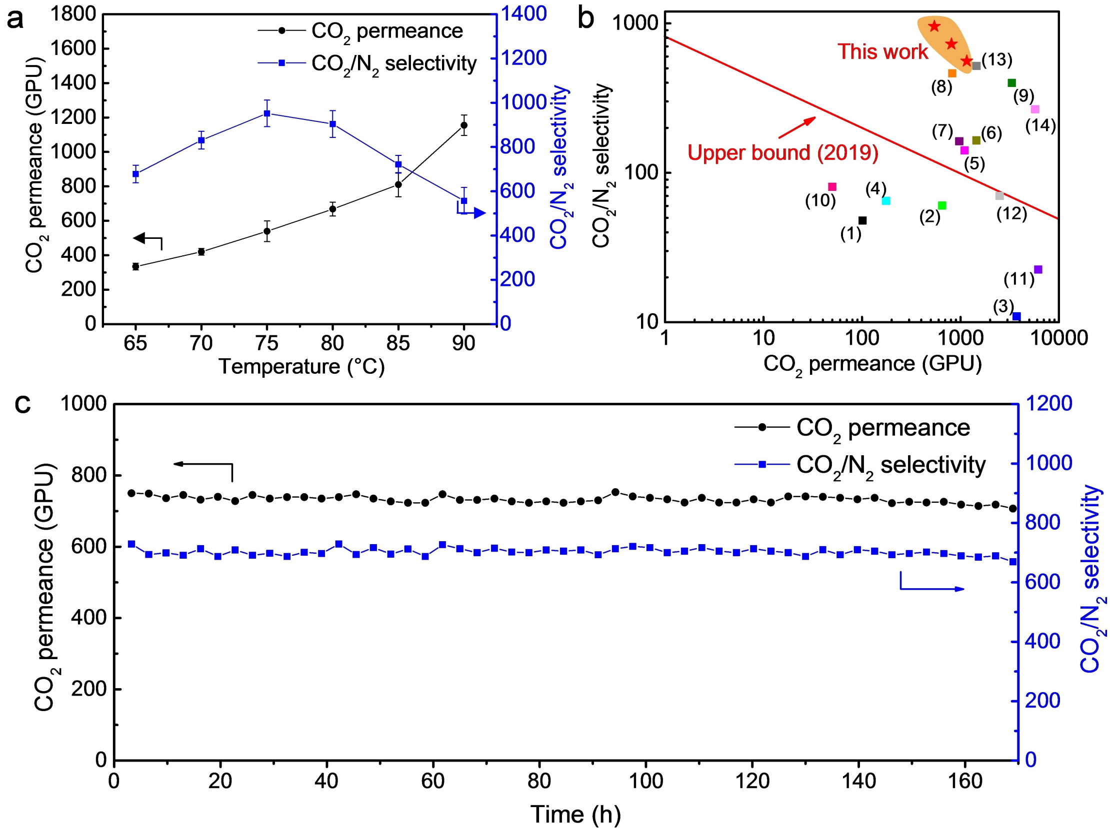

Figure 5. (**a**) CO_2 separation performance of the SCS (80)-DETA (320) membrane at different temperature. (**b**) Comparison of CO_2/N_2 separation performance of our membranes and previously reported polymer membranes and composite membranes: (1) GO membrane,[14] (2) GO-Borate membrane,[15] (3) PDMS membrane,[16] (4) PEG membrane,[17] (5) PVAm-PG membrane,[18] (6) PVAm-PZEA membrane,[19] (7) PZEA-amine membrane,[20] (8) PSS-PEI membrane,[21] (9) PSS-TEPA membrane,[22] (10) PEI@MIL-101(Cr) membrane,[23] (11) nanoporous graphene membrane,[24] (12) GO-amine membrane,[25] (13) NGOQD/SWCNT-DETA membrane,[26] (14) PEIE-HT membrane.[27] Red line: 2019 Robeson upper bound. (**c**) Long-term stability tests of SCS-DETA membrane. The CO_2 separation performance was continuously measured at 85 °C with Ar as sweeping gas.

broad range of membranes, including GO,[14] GO-Borate,[15] PDMS,[16] PEG,[17] PVAm-PG,[18] PVAm-PZEA,[19] PZEA-amine,[20] PSS-PEI,[21] PSS-TEPA,[22] PEI@MIL-101(Cr),[23] nanoporous graphene membranes,[24] GO-amine,[25] NGOQD/SWCNT-DETA[26] and PEIE-HT membranes.[27]

Conclusions

In summary, this work provides a new design concept for FTMs that can achieve efficient CO_2 separation in simulated flue gas. In this structure, mobile amine carriers were stabilized cross-linked SCS gel matrix through the negatively charged sulfonic acid groups, providing abundant facilitated transport sites for effective and stable CO_2 capture. The SCS-DETA gel membrane is capable of separating CO_2 effectively when tested under simulated flue gas conditions. It exhibits a CO_2 permeance of 1155 GPU and an ultra-high CO_2/N_2 selectivity of above 550. The membrane maintained a stable separation performance during the 170 hour continuous test due to the strong electrostatic interaction between the carriers and the SCS gel matrix, indicating their great potential in energy and cost-efficient CO_2 capture from flue gases.

Experimental Section

Materials

The polyether sulfone (PES) microfiltration substrate with an average pore size of 0.45 μm was purchased from Yibo Co., Ltd. (Haining, China). The high-purity single-walled CNT powder (OD: 1–2 nm; length: 5–30 μm; purity: >95%) was purchased from XFNANO. Chitosan (CS, deacetylation degree ≥95%) and diethylenetriamine (DETA, >99%) were purchased from Aladdin. Sodium dodecylbenzenesulfonate (SDBS, >95%) was purchased from J&K Scientific. 1,3-propanesultone (1,3-PS, >99%) was supplied by Meryer. Dopamine hydrochloride, 2-Amino-2-(hydroxylmethyl)-propane-1,3-diol (Tris, >99.9%) and Glutaric dialdehyde (GA, 50% in H_2O) were acquired from Sigma-Aldrich. All chemicals were used in this study and were not further purified.

Fabrication of CNT Network Substrate

The CNT dispersion solution was prepared according to previous reports.[13] 10 mg CNT powder and 100 mg sodium dodecyl benzene sulfonate were added into 100 mL deionized water and sonicated for 10 h under a power of 15 W. After sonication, the CNT dispersion was centrifuged for 30 min at 8000 rpm, and the supernatant dispersion was collected. The concentration of CNT in the dispersion was weighted to be around 0.06 mg mL^{-1}. To enhance its hydrophilicity, CNT was modified by polydopamine. In detail, 10 mg dopamine hydrochloride was added into 100 mL 0.02 mg mL^{-1} CNT dispersion. After stirring for 1 h, 10 mL HCl-Tris buffer solution (10 mM, pH = 7.5) was added into the mixed dispersion and stirred at 40 °C for 24 h. The polydopamine-modified CNT was used in the following experiments. The CNT network substrate was prepared through vacuum filtering 2 mL polydopamine-modified CNT dispersion onto a PES support (pore size: 0.22 μm, diameter: 47 mm). After vacuum filtration, the CNT network substrate was dried in an oven at 60 °C for 30 min.

Synthesis of SCS

The SCS was prepared following the reported work.[28] Firstly, 3 g of CS was added in 200 mL 1 wt% acetic acid solution, and was stirred at 40 °C for 1 h. Secondly, 5 mL 1,3-propanesultone was added dropwise into CS solution under nitrogen atmosphere, and the resulting mixture was stirred at 60 °C for 6 h. Finally, the solution was slowly poured into a cold acetone solution to precipitate white precipitates. After washing the solid with methanol three times, it was dried in an oven for 24 hours to yield white powdered SCS.

Fabrication of SCS-Amine Membranes

The SCS-amine membranes were prepared using a simple spin-coating method on the CNT network substrate. Firstly, 0.027 mL glutaraldehyde (50 % in water) was added into 1 mL 80 mg mL^{-1} SCS solution to form spin-coating solution. Then spin-coating solution should be used within 1 min after mixture. Secondly, 1 mL as-prepared solution was spin-coated on the CNT network substrate at 3000 rpm for 40 s. Then the membrane was kept at room temperature for 30 min to form crosslinked SCS gel membrane. Last, 1 mL 320 mg mL^{-1} DETA solution was spin-coated on the crosslinked SCS gel membrane at 3000 rpm for 40 s.

Gas Separation

The separation performance of CNT/SCS-amine membranes were tested using a simple gas sweeping method. The composite membranes were installed in a stainless-steel infiltration unit in a constant temperature oven. On the feed side, a mixture gas of 10 % CO_2 and 90 % N_2 was used as the simulated flue gas. The flow rate was controlled by mass flow meter 1. Before entering the gas permeation unit, a humidifier was used to saturate the water vapor, allowing it to enter the cell along with the CO_2/N_2 mixture. On the permeation side, Ar as the sweep gas was introduced, and the flow rate was controlled by mass flow meter 2. Permeate gases were brought into GC for composition analysis through Ar.

The gas permeance (P_i of gas i) was calculated by Eq. (1):

$$P_i = V_i/(S \times \Delta P) \tag{1}$$

where V_i is the molar flow rate of component i through the membrane (mol/s), S is the membrane area (m^2), and $\triangle P$ is the transmembrane pressure difference for component i (Pa).

The selectivity of the CO_2/N_2 was calculated by Eq. (2):

$$\alpha = P_{CO_2}/P_{N_2} \tag{2}$$

Supporting Information

Supporting Information is available from the Wiley Online Library or from the author.

Acknowledgements

This work was supported by the National Key Research and Development Program of China (2022YFB3805903), the National Natural Science Foundation of China (22208229, 21988102), the Natural Science Foundation of Jiangsu Province (BK20220501), the Key Research and Development Plan of Jiangsu Province (BE2022056) and Gusu Innovation and Entrepreneurship Leading Talent Plan (ZXL2023198).

Conflict of Interests

The authors declare no conflict of interest.

Data Availability Statement

The data that support the findings of this study are available from the corresponding author upon reasonable request.

Keywords: carbon capture · CO_2 separation membrane · facilitated transport · mobile carrier · sulfonated chitosan gel

[1] a) M. L. Alcantara, G. de Almeida Oliveira, L. M. Lião, C. P. Borges, S. Mattedi, *Ind. Eng. Chem. Res.* **2021**, *60*, 4405–4419; b) S. Kasahara, E. Kamio, T. Ishigami, H. Matsuyama, *Chem. Commun.* **2012**, *48*, 6903–6905; c) E. Shevchenko, A. A. Park, S. Sun, T. Zhang, *Nanoscale* **2023**, *15*, 855–858; d) R.-S. Liu, X.-D. Shi, C.-T. Wang, Y.-Z. Gao, S. Xu, G.-P. Hao, S. Chen, A.-H. Lu, *ChemSusChem* **2021**, *14*, 1428.

[2] a) B. Wang, J. Xu, J. Wang, S. Zhao, X. Liu, Z. Wang, *J. Membr. Sci.* **2021**, *625*, 119175; b) Z. Qiao, S. Zhao, J. Wang, S. Wang, Z. Wang, M. D. Guiver, *Angew. Chem. Int. Ed.* **2016**, *55*, 9321; c) T. Huang, Z. Su, K. Hou, J. Zeng, H. Zhou, L. Zhang, S. P. Nunes, *Chem. Soc. Rev.* **2023**, *52*, 4173–4207; d) J. J. Vericella, S. E. Baker, J. K. Stolaroff, E. B. Duoss, J. O. Hardin, J. Lewicki, E. Glogowski, W. C. Floyd, C. A. Valdez, W. L. Smith, J. H. Satcher Jr, W. L. Bourcier, C. M. Spadaccini, J. A. Lewis, R. D. Aines, *Nat. Commun.* **2015**, *6*, 6124; e) A. Raksajati, M. T. Ho, D. E. Wiley, *Energy Procedia* **2017**, *114*, 764–770.

[3] a) W. F. Yong, F. Y. Li, Y. C. Xiao, T. S. Chung, Y. W. Tong, *J. Membr. Sci.* **2013**, *443*, 156–169; b) N. B. McKeown, *Nat. Mater.* **2016**, *15*, 706–707; c) P. Shao, R. Yao, G. Li, M. Zhang, S. Yuan, X. Wang, Y. Zhu, X. Zhang, L. Zhang, X. Feng, B. Wang, *Angew. Chem. Int. Ed.* **2020**, *59*, 4401–4405; d) H. W. H. Lai, F. M. Benedetti, J. M. Ahn, A. M. Robinson, Y. Wang, I. Pinnau, Z. P. Smith, Y. Xia, *Science* **2022**, *375*, 1390–1392.

[4] a) G. Yu, X. Zou, L. Sun, B. Liu, Z. Wang, P. Zhang, G. Zhu, *Adv. Mater.* **2019**, *31*, 1806853; b) Y. Chen, L. Zhao, B. Wang, P. Dutta, W. S. W. Ho, *J. Membr. Sci.* **2016**, *497*, 21–28; c) W. Luo, Z. Niu, P. Mu, J. Li, *Colloids Surf. A* **2022**, *640*, 128481; d) Y. Han, D. Wu, W. S. W. Ho, *J. Membr. Sci.* **2018**, *567*, 261–271; e) J. Dechnik, J. Gascon, C. J. Doonan, C. Janiak, C. J. Sumby, *Angew. Chem. Int. Ed.* **2017**, *56*, 9292–9310.

[5] a) Z. Guo, H. Wu, Y. Chen, S. Zhu, H. Jiang, S. Song, Y. Ren, Y. Wang, X. Liang, G. He, Y. Li, Z. Jiang, *Angew. Chem. Int. Ed.* **2022**, *61*, 10466; b) Y. Zhang, L. Ma, Y. Lv, T. Tan, *Chem. Eng. J.* **2022**, *430*, 133001; c) Y. Wang, J. Zhao, S. Zhang, Z. Zhang, Z. Zhu, M. Wang, B. Lyu, G. He, F. Pan, Z. Jiang, *Mater. Horiz.* **2023**, *10*, 5016–5021; d) H. Fan, A. Mundstock, A. Feldhoff, A. Knebel, J. Gu, H. Meng J Caro, *J. Am. Chem. Soc.* **2018**, *140*, 10094–10098.

[6] a) Y. Ying, Z. Zhang, S. B. Peh, A. Karmakar, Y. Cheng, J. Zhang, L. Xi, C. Boothroyd, Y. Lam, C. Zhong, D. Zhao, *Angew. Chem. Int. Ed.* **2021**, *60*, 11318–11325; b) K. Xie, Q. Fu, P. A. Webley, G. G. Qiao, *Angew. Chem. Int. Ed.* **2018**, *57*, 8597–8602; c) Z. Wang, D. Wang, S. Zhang, L. Hu, J. Jin, *Adv. Mater.* **2016**, *28*, 3399–3405.

[7] a) K. Qu, J. Xu, L. Dai, Y. Wang, H. Cao, D. Zhang, Y. Wu, W. Xu, K. Huang, C. Lian, X. Guo, W. Jin, Z. Xu, *Angew. Chem. Int. Ed.* **2022**, *61*, 5481; b) A. He, Z. Jiang, Y. Wu, H. Hussain, J. Rawle, M. E. Briggs, M. A. Little, A. G.

Livingston, A. I. Cooper, *Nat. Mater.* **2022**, *21*, 463–470; c) C. Chen, X. Yan, Y. Wu, S. Liu, X. Zhang, X. Sun, Q. Zhu, H. Wu, B. Han, *Angew. Chem. Int. Ed.* **2022**, *61*, 2607.

[8] Y. Cui, H. Kita, K. Okamoto, *Chem. Commun.* **2003**, *17*, 2154–2155.

[9] a) V. Vakharia, W. Salim, M. Gasda, W. S. W. Ho, *J. Membr. Sci.* **2017**, *533*, 220–228; b) S. Kasahara, E. Kamio, T. Ishigami, H. Matsuyama, *J. Membr. Sci.* **2012**, *415–416*, 168–175; c) Q. Xin, Z. Li, C. Li, S. Wang, Z. Jiang, H. Wu, Y. Zhang, J. Yang, X. Cao, *J. Mater. Chem. A.* **2015**, *3*, 6629–6641.

[10] a) W. Xing, T. Peters, M.-L. Fontaine, A. Evans, P. P. Henriksen, T. Norby, R. Bredesen, *J. Membr. Sci.* **2015**, *482*, 115–119; b) Z. Tong, V. K. Vakharia, M. Gasda, W. S. W. Ho, *React. Funct. Polym.* **2015**, *86*, 111–116.

[11] S. Gao, Y. Zhu, F. Zhang, J. Jian, *J. Mater. Chem. A* **2015**, *3*, 2895.

[12] F. Zhou, H. N. Tien, W. L. Xu, J.-T. Chen, Q. Liu, E. Hicks, M. Fathizadeh, S. Li, M. Yu, *Nat. Commun.* **2017**, *8*, 2107.

[13] Y. Lee, B. Gurkan, *J. Membr. Sci.* **2021**, *638*, 119652.

[14] H. W. Kim, H. W. Yoon, S. M. Yoon, B. M. Yoo, B. K. Ahn, Y. H. Cho, H. J. Shin, H. Yang, U. Paik, S. Kwon, J. Y. Choi, H. B. Park, *Science* **2013**, *342*, 91–95.

[15] S. Wang, Y. Wu, N. Zhang, G. He, Q. Xin, X. Wu, H. Wu, X. Cao, M. D. Guiver, Z. Jiang, *Energy Environ. Sci.* **2016**, *9*, 3107–3112.

[16] P. Li, H. Z. Chen, T.-S. Chung, *J. Membr. Sci.* **2013**, *434*, 18–25.

[17] S. Wang, Y. Xie, G. He, Q. Xin, J. Zhang, L. Yang, Y. Li, H. Wu, Y. Zhang, M. D. Guiver, Z. Jiang, *Angew. Chem. Int. Ed.* **2017**, *56*, 14246–14251.

[18] Y. Chen, W. S. W. Ho, *J. Membr. Sci.* **2016**, *514*, 376–384.

[19] Y. Han, D. Wu, W. S. W. Ho, *J. Membr. Sci.* **2019**, *573*, 476–484.

[20] Y. Han, D. Wu, W. S. W. Ho, *J. Membr. Sci.* **2018**, *567*, 261–271.

[21] H. Li, S. Zhang, B. Sengupta, H. Li, F. Wang, S. Li, M. Yu, *J. Membr. Sci.* **2022**, *657*, 120617.

[22] S. Zhang, H. Li, H. Li, B. Sengupta, S. Zha, S. Li, M. Yu, *Adv. Funct. Mater.* **2020**, *30*, 2002804.

[23] Q. Xin, J. Ouyang, T. Liu, Z. Li, Z. Li, Y. Liu, S. Wang, H. Wu, Z. Jiang, X. Cao, *ACS Appl. Mater. Interfaces* **2015**, *7*, 1065–1077.

[24] G. He, S. Huang, L. F. Villalobos, J. Zhao, M. Mensi, E. Oveisi, M. Rezaei, K. V. Agrawal, *Energy Environ. Sci.* **2019**, *12*, 3305–3312.

[25] F. Zhou, Q. Dong, J.-T. Chen, B. Sengupta, J. Jiang, W. L. Xu, H. Li, S. Li, M. Yu, *Chem. Eng. J.* **2022**, *430*, 132942.

[26] F. Zhou, H. N. Tien, Q. Dong, W. L. Xu, B. Sengupta, S. Zha, J. Jiang, D. Behera, S. Li, M. Yu, *J. Mater. Chem. A* **2020**, *8*, 1084–1090.

[27] J. Liao, Z. Wang, C. Gao, S. Li, Z. Qiao, M. Wang, S. Zhao, X. Xie, J. Wang, S. Wang, *Chem. Sci.* **2014**, *5*, 2843–2849.

[28] Z. Sun, C. Shi, X. Wang, Q. Fang, J. Huang, *Carbohydr. Polym.* **2017**, *155*, 321–328.

Manuscript received: January 24, 2024
Revised manuscript received: April 1, 2024
Accepted manuscript online: April 10, 2024
Version of record online: ■■, ■■

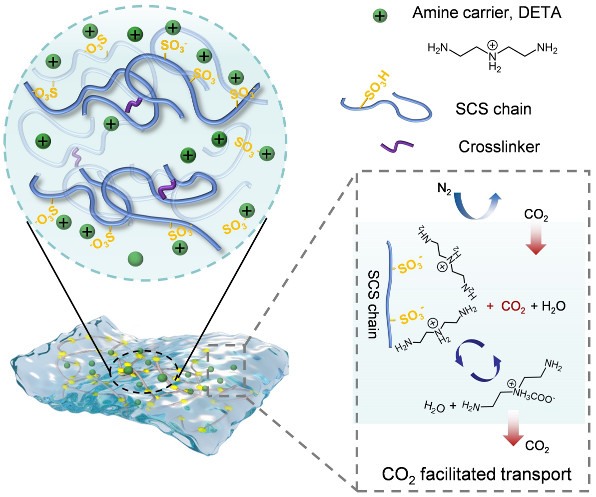

A highly stable, CO_2 facilated transport membrane that can operate at simulated flue gas conditions with temperature up to 90 °C and high humidity is reported. The mobile amine-carriers for CO_2 were stablized within the sulfonated chitosan ion gel membrane. By virtue of carrier-facilitated transport, high CO_2 permeance (as high as 1155 GPU) and ultrahigh CO_2/N_2 selectivity (above 550) were achieved.

L. Wang, Dr. S. Zha, Dr. S. Zhang, Prof. J. Jin**

1 – 9

Sulfonated Chitosan Gel Membrane with Confined Amine Carriers for Stable and Efficient Carbon Dioxide Capture